



Cite this: *Soft Matter*, 2019, 15, 9215

# Elastic properties of liquid-crystalline bilayers self-assembled from semiflexible–flexible diblock copolymers

Yongqiang Cai,<sup>a</sup> Pingwen Zhang<sup>\*b</sup> and An-Chang Shi<sup>id \*c</sup>

The mechanical response and shape of self-assembled bilayer membranes depend crucially on their elastic properties. Most of the studies focused on the elastic properties of fluid membranes, despite the ubiquitous presence of membranes with liquid-crystalline order. Here the elastic properties of liquid-crystalline bilayers self-assembled from diblock copolymers composed of a semiflexible block are studied theoretically. Specifically, the self-consistent field theory (SCFT) is applied to a model system composed of semiflexible–flexible diblock copolymers dissolved in flexible homopolymers that act as solvents. The free energy of self-assembled tensionless bilayer membranes in three different geometries, *i.e.* planar, cylindrical and spherical, is obtained by solving the SCFT equations using a hybrid method, in which the orientation-dependent functions are treated using the spherical harmonics, whereas the position-dependent operators are treated using the compact difference schemes. The bending modulus  $\kappa_M$  and Gaussian modulus  $\kappa_G$  of the bilayer are extracted from the free energies. The effects of the molecular parameters of the system, such as the chain rigidity and the orientational interaction, are systematically examined.

Received 12th September 2019,  
Accepted 16th October 2019

DOI: 10.1039/c9sm01844a

[rsc.li/soft-matter-journal](http://rsc.li/soft-matter-journal)

## 1 Introduction

Understanding the self-assembly of amphiphilic molecules such as lipids to form bilayer membranes is fundamental to many areas including life itself. Macromolecular analogues of lipids, such as amphiphilic block copolymers, could act as mimetics of biological membranes. The study of bilayer membranes self-assembled from amphiphilic block copolymers not only sheds light on the understanding of the fundamentals of self-assembly, but also provides macromolecular analogues of bilayer membranes that have various applications. In particular, polymeric hybrid membranes show a great promise for applications in biomedicine and biotechnology because there are virtually no limits to the selection of monomers and chain architecture.<sup>1</sup>

Phenomenologically, a membrane could be regarded as a two-dimensional surface, whose mechanical properties are characterized by their bending modulus. The deformation mechanics of membranes could be used to understand the formation and stability of membrane morphologies. Assuming

that the deformation is small, the energy of a deformed bilayer could be described by Helfrich's linear elasticity theory.<sup>2,3</sup> Specifically, the Helfrich model states that the elastic energy of a closed membrane is given by,

$$F = \int [\gamma + 2\kappa_M(M - c_0)^2 + \kappa_G G] dA, \quad (1)$$

where  $M = (c_1 + c_2)/2$  and  $G = c_1c_2$  are the local mean and Gaussian curvatures of a deformed bilayer, respectively ( $c_1, c_2$  are the two principal curvatures). The energetics of a bilayer is therefore specified by the elastic constants,  $\gamma, c_0, \kappa_M$  and  $\kappa_G$ , corresponding to the surface tension, spontaneous curvature, the bending modulus and the Gaussian modulus, respectively. For bilayer membranes made of two leaflets with identical composition, the spontaneous curvature  $c_0$  is zero. Because the membranes are formed by the self-assembly of amphiphilic molecules, it is important to understand how the molecular parameters determine the elastic constants of the membranes.

During the last decades, a number of experimental techniques,<sup>4,5</sup> simulation protocols<sup>6–8</sup> and theoretical methods<sup>9–11</sup> have been developed to obtain the elastic constants of bilayer membranes. Theoretically, one method to obtain the elastic constants is by studying bilayers in different geometries (*e.g.*, planes, cylinders, spheres), and comparing the free energy of membranes with different shapes of definite curvatures.<sup>10</sup> This approach can be implemented quite naturally in numerical and theoretical

<sup>a</sup> Department of Mathematics, National University of Singapore, Singapore 119076, Singapore. E-mail: [matcyon@nus.edu.sg](mailto:matcyon@nus.edu.sg)

<sup>b</sup> LMAM, CAPT and School of Mathematical Sciences, Peking University, Beijing 100871, P. R. China. E-mail: [pzhang@pku.edu.cn](mailto:pzhang@pku.edu.cn)

<sup>c</sup> Department of Physics and Astronomy, McMaster University, Hamilton L8S 4M1, Ontario, Canada. E-mail: [shi@mcmaster.ca](mailto:shi@mcmaster.ca)

studies. One requirement of this geometric method is an accurate computation of the free energy of curved membranes, which in turn requires a robust theoretical model of the amphiphilic molecules. Among the different theoretical frameworks developed for amphiphilic molecules, the self-consistent field theory (SCFT) provides a versatile framework for the study of self-assembled bilayer membranes. A number of previous studies using SCFT have been carried out to investigate the elastic properties of self-assembled bilayers.<sup>10,12–14</sup> In almost all of these studies, the polymeric components are assuming to be flexible, and the Gaussian-chain model is used to describe these flexible blocks. On the other hand, many amphiphilic molecules contain a rigid or semiflexible component, thus it is interesting and important to extend these previous studies to non-Gaussian models. In this study, we extend the SCFT of flexible polymers to the semiflexible polymers described by the wormlike-chain model and study the elastic properties of liquid-crystalline bilayers self-assembled from semiflexible-flexible diblock copolymers.

The most significant difference between flexible and semiflexible polymers is that semiflexible polymers could possess orientational or liquid-crystalline order. It is well known that the liquid-crystalline behaviors of semiflexible blocks have significant effects on the self-assembly of semiflexible polymers, such as rod-coil diblock copolymers, in solutions, in melts or confined in thin films.<sup>15–19</sup> For the self-assembled bilayers from rod-coil diblock copolymers, our earlier theoretical study has predicted that a variety of liquid-crystalline bilayers, such as the A-phase and C-phase corresponding to the smectic phases in bulk systems, could become equilibrium phases of the rod-coil/coil system.<sup>20</sup> It is natural to expect that the liquid-crystalline order of the bilayers could have significant effects on the elastic properties of the membranes.

In this paper, we report on a systematic study of the elastic properties of bilayer membranes self-assembled from semiflexible-flexible diblock copolymers using the SCFT. It has been demonstrated that the SCFT provides a flexible and accurate framework for the study of inhomogeneous polymeric systems including different micelle structures.<sup>21,22</sup> In the current study, we obtained accurate numerical solutions of the SCFT equations corresponding to various tensionless liquid-crystalline bilayers constrained in three geometries (plan, cylinder and sphere). The bending modulus and Gaussian modulus are extracted by fitting the free energies of curved bilayers to the Helfrich model. The dependence of the elastic properties on the microscopic parameters of block polymers are studied.

The remainder of this paper is organized as follows. Section 2 describes the SCFT model of our system, the geometric constraints used in this study, the modified diffusion equations in planar, cylindrical and spherical coordinate systems and the numerical methods to solve the proposed model. Our results on the elastic properties of the membranes are presented in Section 3, including the influence of microscopic parameters of the semiflexible-flexible system on the elastic properties. Finally, Section 4 concludes with a brief summary.

## 2 Model and methods

### 2.1 Basic model

The model system used in our study is a binary mixture of A (coil, flexible)–B (semiflexible) diblock copolymers and A (coil) homopolymers. In this model the diblock copolymers act as the amphiphilic molecules and the homopolymers act as the solvents. The phase behaviour of this system is controlled by a large number of parameters related to the molecular properties. In the current study, the copolymers and homopolymers are assumed, for simplicity, to have the same degree of polymerization  $N$ . The volume fraction of the A- and B-blocks of the copolymers are denoted by  $f_A$  and  $f_B = 1 - f_A$ , respectively. The interaction between the A and B monomers is described by a Flory–Huggins parameter<sup>23</sup>  $\chi$ , whereas the orientation interaction between the semiflexible segments is assumed to have the Maier–Saupe form<sup>24</sup> quantified by an interaction parameter  $\eta$ . The rigidity of the semiflexible chain is further measured by a parameter  $\lambda$ . Furthermore, the conformational asymmetry between the A- and B-blocks is quantified by the geometrical asymmetry parameter,<sup>25,26</sup>  $\beta = L/R_g$ , where  $L = bN$  is the total polymer-contour,  $R_g = \sqrt{Na^2/6}$  is the gyration radius of the A-chains,  $a$  and  $b$  are the statistical segment lengths of A and B blocks, respectively. Finally the chemical potential of the copolymers  $\mu_c$ , or the corresponding activity  $z_c = \exp(\mu_c)$  is used to control the average concentration of the diblock copolymers in the system.

Within the SCFT framework formulated in the grand canonical ensemble,<sup>20</sup> the free energy of the binary mixture is given by,

$$\begin{aligned} \frac{N\mathcal{F}}{k_B T \rho_0} = & \int d\mathbf{r} [\chi N \phi_A(\mathbf{r}) \phi_B(\mathbf{r}) - \omega_A(\mathbf{r}) \phi_A(\mathbf{r}) - \omega_B(\mathbf{r}) \phi_B(\mathbf{r}) \\ & + \frac{1}{2\eta N} \mathbf{M}(\mathbf{r}) : \mathbf{M}(\mathbf{r}) - \zeta(\mathbf{r}) (\phi_A(\mathbf{r}) + \phi_B(\mathbf{r}) - 1) \\ & + \psi G_\varepsilon(\mathbf{r} - \mathbf{r}_1) (\phi_A(\mathbf{r}) - \phi_B(\mathbf{r}))] - z_c Q_c - Q_h, \end{aligned} \quad (2)$$

where  $\phi_\alpha(\mathbf{r})$  and  $\omega_\alpha(\mathbf{r})$  are the local concentration and the mean field of the  $\alpha$ -type monomers ( $\alpha = A, B$ ). The tensor field  $\mathbf{M}(\mathbf{r})$  is the mean orientation field of the semiflexible blocks (B). The local pressure field  $\zeta(\mathbf{r})$  is a Lagrange multiplier introduced to enforce incompressibility of the system. A second Lagrange multiplier,  $\psi$ , is used to stabilize the bilayer of different geometries. Here a sharp Gaussian with width  $\varepsilon$ ,  $G_\varepsilon(\mathbf{r} - \mathbf{r}_1)$ , is used to ensure that the  $\psi$  field only operates near the interface at a prescribed position  $\mathbf{r}_1$ . The last two terms in eqn (2) are the contributions from the single-chain partition functions of the two polymers,  $Q_c$  and  $Q_h$ .

The fundamental quantity to be calculated in the SCFT is the polymer segment probability distribution functions (or the propagators),  $q_A^h(\mathbf{r}, s)$  for the A-homopolymers, and  $q_A^\pm(\mathbf{r}, s)$ ,  $q_B^\pm(\mathbf{r}, \mathbf{u}, s)$  for the AB-diblock copolymers, where  $\mathbf{u}$  is an unit orientational vector. These propagators satisfy the modified diffusion equations (MDE)<sup>21</sup> in the presence of the mean fields ( $\omega_A$ ,  $\omega_B$  and  $\mathbf{M}$ ),

$$\frac{\partial}{\partial s} q_A^h(\mathbf{r}, s) = (R_g^2 \nabla_{\mathbf{r}}^2 - \omega_A(\mathbf{r})) q_A^h(\mathbf{r}, s), \quad s \in (0, 1), \quad (3)$$

$$\frac{\partial}{\partial s} q_A^\pm(\mathbf{r}, s) = (R_g^2 \nabla_{\mathbf{r}}^2 - \omega_A(\mathbf{r})) q_A^\pm(\mathbf{r}, s), \quad s \in (0, f_A), \quad (4)$$

$$\frac{\partial}{\partial s} q_B^\pm(\mathbf{r}, \mathbf{u}, s) = \left( \pm \beta R_g \mathbf{u} \cdot \nabla_{\mathbf{r}} |_{\mathbf{u}} - \Gamma(\mathbf{r}, \mathbf{u}) + \frac{L}{2\lambda} \nabla_{\mathbf{u}}^2 \right) q_B^\pm(\mathbf{r}, \mathbf{u}, s), \quad s \in (0, f_B), \quad (5)$$

with the initial conditions,

$$q_A^h(\mathbf{r}, 0) = q_A^-(\mathbf{r}, 0) = 1, \quad q_B^-(\mathbf{r}, \mathbf{u}, 0) = \frac{1}{4\pi}, \quad (6)$$

$$q_A^+(\mathbf{r}, 0) = \int d\mathbf{u} q_B^-(\mathbf{r}, \mathbf{u}, f_B), \quad q_B^+(\mathbf{r}, \mathbf{u}, 0) = \frac{1}{4\pi} q_A^-(\mathbf{r}, f_A). \quad (7)$$

The  $\mathbf{r}, \mathbf{u}$ -dependent field  $\Gamma(\mathbf{r}, \mathbf{u})$  is defined by

$$\Gamma(\mathbf{r}, \mathbf{u}) = \omega_B(\mathbf{r}) - \mathbf{M}(\mathbf{r}) : \left( \mathbf{u} \mathbf{u} - \frac{1}{3} \mathbf{I} \right). \quad (8)$$

In terms of the chain propagators, the single-chain partition functions are given by,

$$Q_c = \int d\mathbf{r} q_A^+(\mathbf{r}, f_A), \quad (9)$$

$$Q_h = \int d\mathbf{r} q_A^h(\mathbf{r}, 1). \quad (10)$$

Furthermore, the density distributions of the A- and B-monomers are obtained from the propagators as,

$$\begin{aligned} \phi_A(\mathbf{r}) &= \phi_A^h + \phi_A^c = \int_0^1 ds q_A^h(\mathbf{r}, s) q_A^h(\mathbf{r}, 1-s) \\ &+ z_c \int_0^{f_A} ds q_A^-(\mathbf{r}, s) q_A^+(\mathbf{r}, f_A-s), \end{aligned} \quad (11)$$

$$\phi_B(\mathbf{r}) = 4\pi z_c \int_0^{f_B} ds \int d\mathbf{u} q_B^-(\mathbf{r}, \mathbf{u}, s) q_B^+(\mathbf{r}, \mathbf{u}, f_B-s). \quad (12)$$

Finally the orientational order parameter of the B-blocks is given by

$$\mathbf{S}(\mathbf{r}) = 4\pi z_c \int_0^{f_B} ds \int d\mathbf{u} q_B^-(\mathbf{r}, \mathbf{u}, s) \left( \mathbf{u} \mathbf{u} - \frac{1}{3} \mathbf{I} \right) q_B^+(\mathbf{r}, \mathbf{u}, f_B-s). \quad (13)$$

The rest of the SCFT equations relating the mean fields to the density distributions are,

$$\omega_A(\mathbf{r}) = \chi N \phi_B(\mathbf{r}) - \zeta(\mathbf{r}) + \psi G_\varepsilon(\mathbf{r} - \mathbf{r}_1), \quad (14)$$

$$\omega_B(\mathbf{r}) = \chi N \phi_A(\mathbf{r}) - \zeta(\mathbf{r}) - \psi G_\varepsilon(\mathbf{r} - \mathbf{r}_1), \quad (15)$$

$$\mathbf{M}(\mathbf{r}) = \eta \mathbf{N} \mathbf{S}(\mathbf{r}), \quad (16)$$

$$\phi_A(\mathbf{r}) + \phi_B(\mathbf{r}) = 1, \quad (17)$$

$$\int d\mathbf{r} G_\varepsilon(\mathbf{r} - \mathbf{r}_1) (\phi_A(\mathbf{r}) - \phi_B(\mathbf{r})) = 0. \quad (18)$$

We are interested in the free energy of a system containing a bilayer membrane compared to that of the homogeneous bulk phase  $\mathcal{F}_{\text{bulk}}$ , which can be computed analytically by solving SCF equations with constant functions.<sup>14,27</sup> The free energy difference

$(\mathcal{F} - \mathcal{F}_{\text{bulk}})$  is proportional to the area of the membrane A, therefore we can define an excess free energy density as,

$$F_{\text{ex}} = \frac{N(\mathcal{F} - \mathcal{F}_{\text{bulk}})}{k_B T \rho_0 A}. \quad (19)$$

The free energy for the bulk phase is given by,

$$\frac{N\mathcal{F}_{\text{bulk}}}{k_B T \rho_0 V} = \chi N f_B^2 \phi_{\text{bulk}}^2 + \ln(1 - \phi_{\text{bulk}}) - 1, \quad (20)$$

where the bulk copolymer concentration  $\phi_{\text{bulk}}$  is determined by the following equation,

$$\mu_c = \ln \phi_{\text{bulk}} - \ln(1 - \phi_{\text{bulk}}) + \chi N f_B (1 - 2f_B \phi_{\text{bulk}}). \quad (21)$$

## 2.2 Geometrical constraints

In order to extract the elastic parameters of the bilayer, especially the bending modulus and Gaussian modulus, we need to calculate the excess free energy of deformed bilayer membranes. Specifically, we compute the free energy of the bilayers in three geometries: an infinite planar bilayer, a cylindrical bilayer with a radius  $r$ , which is extended to infinity in the axial direction, and a spherical bilayer with a radius  $r$ . In previous studies,<sup>14,28</sup> a constraint term,  $\delta(\mathbf{r} - \mathbf{r}_1)(\phi_A(\mathbf{r}) - \phi_B(\mathbf{r}))$ , has been included in the free energy functional to stabilize a bilayer in those geometries. In the cylindrical and spherical geometries, the constraint is applied to the outer monolayer only which allows the bilayer to optimise its thickness and indirectly sets the curvature radius of the membrane. In this paper we treat the delta function  $\delta(\mathbf{r})$  as the limit of the Gaussian function,  $G_\varepsilon(\mathbf{r})$ , with  $\varepsilon$  tending to zero, and use a more moderate constraint term,  $G_\varepsilon(\mathbf{r} - \mathbf{r}_1)(\phi_A(\mathbf{r}) - \phi_B(\mathbf{r}))$ , in eqn (2). Mathematically, replacing the delta function with a Gaussian function improves the numerical stability. It should also be noted that there is a convection term in the MDE of the wormlike chain and many numerical methods for convection equation could involve a loss of precision when the solution is not smooth. Hence using the Gaussian function  $G_\varepsilon$  could avoid potential numerical problems.

With these geometrical constraints, we obtained the excess free energies for the three geometries, which are denoted by  $F^0$ ,  $F^C$ ,  $F^S$  for the planar, cylindrical and spherical membranes, respectively. In this work, we focus on the tensionless bilayer membranes, and the chemical potential of the copolymer,  $\mu_c$ , is adjusted such that the excess free energy of a planar bilayer is zero, *i.e.*  $F^0 = \gamma + 2\kappa_M c_0^2 = 0$ , which is equivalent to  $\gamma = 0$  for a bilayer membrane consisting of two identical leaflets has its spontaneous curvature  $c_0$  to be zero by symmetry.<sup>14</sup> For a curved bilayer of finite thickness, the definition of the interface position involves a certain degree of arbitrariness. We define the bilayer interface,  $r$ , to be at the mid-point of the two position where A- and B-segment concentrations are equal. The Helfrich free energy can be written in terms of the curvature  $c = 1/r$  in the cylindrical and spherical geometries,

$$F^C(c) = F^0 - 2\kappa_M c_0 c + \frac{\kappa_M}{2} c^2 = \frac{\kappa_M}{2} c^2, \quad (22)$$

$$F^S(c) = F^0 - 4\kappa_M c_0 c + (2\kappa_M + \kappa_G) c^2 = (2\kappa_M + \kappa_G) c^2. \quad (23)$$

The bending modulus  $\kappa_M$  and Gaussian modulus  $\kappa_G$  can be obtained by quadratic polynomial fitting the effect of the curvature  $c$  on the excess free energy  $F^C$  and  $F^S$ .

### 2.3 MDEs in cylindrical and spherical coordinate systems

When the internal structure of the bilayer is disordered or ordered with rotational symmetry, the above three geometries can be reduced to a one-dimensional problem by an appropriate coordinate transformation. Specifically, the MDE for coils in one-dimensional planar, cylindrical and spherical coordinate systems can be written in a unified form,

$$\frac{\partial}{\partial s} q(r, s) = R_g^2 \frac{1}{r^n} \frac{\partial}{\partial r} \left( r^n \frac{\partial}{\partial r} q(r, s) \right) - \omega(r) q(r, s), \quad (24)$$

where  $n = 0, 1, 2$  for planar, cylindrical and spherical coordinate systems respectively. The situation for semiflexible chain is more complicated since the orientation of the semiflexible segments is coupled with its spatial coordinates. The MDE for propagator  $q(\mathbf{r}, \mathbf{u}, s)$  of semiflexible chain in curvilinear coordinates is,<sup>29</sup>

$$\frac{\partial q}{\partial s} = \pm \beta R_g (\mathbf{u} \cdot \nabla_{\mathbf{r}} - [(\mathbf{u} \cdot \nabla) \mathbf{u}] \cdot \nabla_{\mathbf{u}}) q - \Gamma(\mathbf{r}, \mathbf{u}) q + \frac{L}{2\lambda} \nabla_{\mathbf{u}}^2 q. \quad (25)$$

Our previous study<sup>20</sup> demonstrated that rod-coil diblock planar bilayers could possess liquid-crystalline phase, such as A-phase, OB-phase, C-phase, and P-phase. Of these four phases, a bilayer membrane can be curved to a symmetrical cylinder, but only the A-phases and OB-phase can be curved to a rotation symmetrical sphere. In planar coordinate systems, the unit orientation vector at  $\mathbf{r} = (x, y, z)$  expressed as,  $\mathbf{u} = \sin \Theta \cos \Phi \mathbf{e}_x + \sin \Theta \sin \Phi \mathbf{e}_y + \cos \Theta \mathbf{e}_z$ , and the one-dimensional MDE for  $q(\mathbf{r}, \mathbf{u}, s)$  is,

$$\frac{\partial q}{\partial s} = \pm \beta R_g \cos \Theta \frac{\partial q}{\partial r} - \Gamma(r, \mathbf{u}) q + \frac{L}{2\lambda} \nabla_{\mathbf{u}}^2 q = :L_P q. \quad (26)$$

Here the right hand is the operation of operator  $L_P = \pm \beta R_g \cos \Theta \partial_r - \Gamma(r, \mathbf{u}) + \frac{L}{2\lambda} \nabla_{\mathbf{u}}^2$  on propagator  $q$ , and the variable  $x$  is rewritten by  $r$ .

The coordinate in cylindrical coordinate systems is  $\mathbf{r} = (r, \phi, z)$ , and the unit orientation vector  $u$  is defined by  $\mathbf{u} = \sin \Theta \cos \Phi \mathbf{e}_\phi + \sin \Theta \sin \Phi \mathbf{e}_z + \cos \Theta \mathbf{e}_r$ . Rewrote  $q(\mathbf{r}, \mathbf{u}, s)$  by  $q(\phi, z, r, \Theta, \Phi, s)$ , the symmetrical propagator  $q(r, \Theta, \Phi, s)$  satisfy the one-dimensional MDE,

$$\frac{\partial q}{\partial s} = \pm \beta R_g \left( -\frac{\sin \Theta \cos^2 \Phi}{r} \frac{\partial q}{\partial \Theta} + \frac{\cos \Theta \sin 2\Phi}{2r} \frac{\partial q}{\partial \Phi} \right) + L_P q. \quad (27)$$

Similarly, the coordinate in spherical coordinate systems is  $\mathbf{r} = (r, \theta, \phi)$ , unit orientation vector is defined by  $\mathbf{u} = \sin \Theta \cos \Phi \mathbf{e}_\theta + \sin \Theta \sin \Phi \mathbf{e}_\phi + \cos \Theta \mathbf{e}_r$ , and the MDE for  $q(r, \Theta, \Phi, s)$  is

$$\frac{\partial q}{\partial s} = \pm \beta R_g \left( -\frac{\sin \Theta}{r} \frac{\partial q}{\partial \Theta} - \frac{\sin \Theta \sin \Phi \cos \theta}{r \sin \theta} \frac{\partial q}{\partial \Phi} \right) + L_P q. \quad (28)$$

Note that the coefficient before  $\frac{\partial q}{\partial \Phi}$  is depend on  $\theta$ , which indicate that a orientational symmetrical solution  $q(r, \Theta, \Phi, s)$  must independent on  $\Phi$ . Thus the one-dimensional MDE for  $q(r, \Theta, s)$  is,

$$\frac{\partial q}{\partial s} = \pm \beta R_g \left( -\frac{\sin \Theta}{r} \frac{\partial q}{\partial \Theta} \right) + L_P q. \quad (29)$$

### 2.4 Numerical method

For a given set of control parameters, the above SCFT equations are solved to obtain solutions corresponding to bilayers of different geometries. Numerically, the SCFT equations are solved by iteration, and accelerated convergence by Anderson mixing.<sup>30</sup> The most time-consuming step is to compute the propagators by solving the diffusion-like equations, especially for the semiflexible chain. Using operator splitting method, we divided the solving MDE for semiflexible chain into two subproblems, one for the spatial domain and another for the orientation,

$$\frac{\partial q_1}{\partial s} = \pm \beta R_g \cos \Theta \frac{\partial q_1}{\partial r} - \Gamma(r, \mathbf{u}) q_1, \quad (30)$$

$$\frac{\partial q_2}{\partial s} = \mp \beta R_g [(\mathbf{u} \cdot \nabla) \mathbf{u}] \cdot \nabla_{\mathbf{u}} q_2 + \frac{L}{2\lambda} \nabla_{\mathbf{u}}^2 q_2. \quad (31)$$

In this study, the MDEs are supplemented with reflecting boundary conditions, and the eqn (24) and (31) are solved using the compact finite difference schemes.<sup>31</sup> In particular, the partial derivative operators about  $\mathbf{r}$  are treated by a fourth-order compact finite difference schemes, and the  $s$  dependence is dealt by implicit Runge-Kutta method.<sup>32</sup> The scheme is especially suitable for the current problem where a well-designed nonuniform grid is easily used to capture the sharp interface. The MDE (31) is solved by spectral method employing the spherical harmonics as basic functions. The spherical harmonics are defined as,

$$Y_l^m(\Theta, \Phi) = \sqrt{\frac{2l+1}{4\pi} \frac{(l-m)!}{(l+m)!}} P_l^m(\cos \Theta) e^{im\Phi}, \quad (32)$$

$$l \geq 0, |m| \leq l,$$

where  $P_l^m$  is the associated Legendre polynomials. The spherical harmonics are eigenfunctions of the Laplacian operator,  $\nabla_{\mathbf{u}}^2$ , and have relation,  $\nabla_{\mathbf{u}}^2 Y_l^m = -l(l+1) Y_l^m$ . To express the operation of the first term in right hand of eqn (31), (27) and (29) on spherical harmonics, we define two operators  $L_C$  and  $L_S$ ,

$$L_C = -\sin \Theta \cos^2 \Phi \partial_\Theta + \cos \Theta \sin \Phi \cos \Phi \partial_\Phi, \quad (33)$$

$$L_S = -\sin \Theta \partial_\Theta. \quad (34)$$

Their operations on  $Y_l^m$  can be expressed by several spherical harmonics,

$$L_C Y_l^m = a_{l,m}^- Y_{l-1}^m + a_{l,m}^+ Y_{l+1}^m + b_{l,m}^- Y_{l-1}^{m-2} + b_{l,m}^+ Y_{l+1}^{m-2} + c_{l,m}^- Y_{l-1}^{m+2} + c_{l,m}^+ Y_{l+1}^{m+2}, \quad (35)$$

$$L_S Y_l^m = 2a_{l,m}^- Y_{l-1}^m + 2a_{l,m}^+ Y_{l+1}^m. \quad (36)$$

Here  $Y_l^m = 0$  for  $l < 0$  or  $|m| > l$ , and the coefficients are,

$$\begin{aligned} a_{lm}^- &= \frac{l+1}{2} \sqrt{\frac{l^2-m^2}{4l^2-1}}, \\ a_{lm}^+ &= -\frac{l}{2} \sqrt{\frac{(l+1)^2-m^2}{4(l+1)^2-1}}, \\ b_{lm}^- &= -\frac{1}{4} \sqrt{\frac{(l-m+1)(l+m-2)(l+m-1)(l+m)}{4l^2-1}}, \\ b_{lm}^+ &= \frac{1}{4} \sqrt{\frac{(l-m+1)(l-m+2)(l-m+3)(l+m)}{4(l+1)^2-1}}, \\ c_{lm}^- &= -\frac{1}{4} \sqrt{\frac{(l+m+1)(l-m-2)(l-m-1)(l-m)}{4l^2-1}}, \\ c_{lm}^+ &= \frac{1}{4} \sqrt{\frac{(l+m+1)(l+m+2)(l+m+3)(l-m)}{4(l+1)^2-1}}. \end{aligned}$$

Expanding  $\mathbf{u}$ -dependent functions in terms of spherical harmonics,

$$q(\Theta, \Phi, s) = \sum_{l,m} \hat{q}_{lm}(s) Y_l^m(\Theta, \Phi), \quad (37)$$

the modified diffusion eqn (31), specified in cylindrical and spherical coordinate systems, is converted to linear ordinary differential equations (ODE) respect to spherical harmonic coefficients  $\hat{q}_{lm}$ . This ODE has a constant and sparse coefficient matrix, which can be solved efficiently.

In the current study, the gyration radius  $R_g$  is set as the unit length, *i.e.*  $R_g = 1$ , the numerical domain is constraint to one dimensional and the size is determined by the concentration profile to ensure the order near boundary is close to the bulk phase. The orientation vector  $\mathbf{u}$  on unit sphere is discretized by 32 values of  $\Theta$  and 36 values of  $\Phi$ , and the spherical harmonics expansion (37) is truncated by  $|m| \leq l \leq 16$ . The number of spatial grid point is changed over 200–400, and time grid point over 300–800 under different model parameters to make sure the free energy is converged in the order of  $10^{-4}$  and the fields are self-consistent with  $L^2$ -norm error less than  $10^{-6}$ . The Gaussian width  $\varepsilon$  in eqn (2) is set as  $\varepsilon = 0.2R_g$ . (However, the elastic parameters are insensitive to the constraint Gaussian width  $\varepsilon$ .)

## 3 Results and discussion

### 3.1 Cylindrical and spherical bilayers

From the SCFT free energy of cylindrical and spherical membranes with large radii or small curvatures, the bending modulus and the Gaussian modulus can be calculated by fitting the free energy curve to the Helfrich model. The basic structural properties of a self-assembled bilayer membrane are the spatial distribution of the hydrophilic and hydrophobic monomers across it, and the liquid-crystalline order of the semiflexible monomers. A typical concentration profile for the A-phase liquid-crystalline bilayer membrane in the spherical and cylindrical geometry with the radius near  $r = 6R_g$  is shown in Fig. 1. Similar to the flexible bilayer membrane,<sup>14</sup> the hydrophilic monomers (A-blocks) in the inner leaflet have to pack more closely and

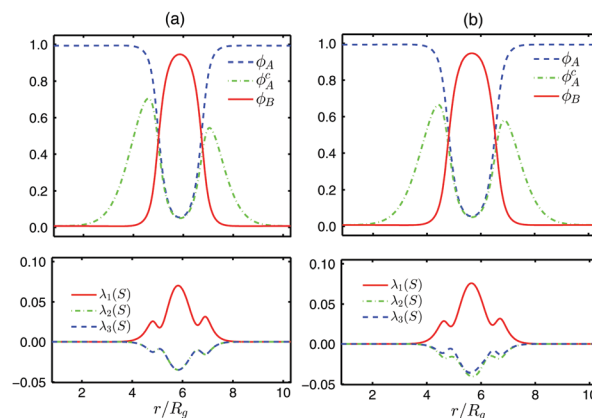


Fig. 1 Concentration profiles of an A-phase (a) spherical and (b) cylindrical bilayer membrane ( $\chi N = \eta N = 15$ ,  $\beta = 4$ ,  $\lambda/L = 1.5$ ,  $f_A = 0.5$ ).  $\lambda_i(S)$  are the eigenvalues of  $S$ .

have a higher local concentration and wider distribution in the axial direction, in comparison to the outer leaflet. In the spherical A-phase bilayer, the orientation of the semiflexible blocks are uniaxial because the geometry is isotropic, therefore the orientation order parameter  $S$  has repeated eigenvalues, *i.e.*  $\lambda_2(S) = \lambda_3(S) = -\frac{1}{2}\lambda_1(S)$ . However, the cylinder has different principal curvatures, hence the orientation in the cylindrical bilayer has a little divergence from uniaxial distribution, *i.e.*  $\lambda_2(S) \neq \lambda_3(S)$  (see Fig. 1(b)).

### 3.2 Influence of chain rigidity

The semiflexible or wormlike chain model are specified by two independent parameters, the total contour length  $L$  and the chain rigidity parameter  $\lambda$ . The mean-squared end-to-end vector for the wormlike chain is given by,<sup>21</sup>

$$R^2 = L^2 \frac{2\lambda}{L} \left[ 1 - \frac{\lambda}{L} (1 - e^{-L/\lambda}) \right]. \quad (38)$$

This expression could be continuously interpolated between the properties of a flexible, ideal chain and a rigid rod. In the flexible limit,  $L/\lambda \gg 1$ ,  $R$  reduces to  $R \approx \sqrt{2}\lambda\sqrt{L/\lambda}$ , which is consistent with the ideal chain scaling formula  $R = b\sqrt{N}$  for freely jointed chains if we choose to interpret  $N = L/\lambda$  as the number of statistically independent persistent segments and select  $b = \sqrt{2}\lambda$ . In the opposite limit of  $L/\lambda \ll 1$ ,  $R$  reduces to  $R \approx L$  which is evidently the exact result for a rigid rod. With  $\lambda/L$  changes from zero to infinity, the wormlike chain model can describe both the coils and rigid rods. Here, we investigate the effect of the rigidity of wormlike chain on the elastic properties of semiflexible-coil bilayer membranes.

In order to cover the different scaling ratio, we fixed the mean-squared end-to-end vector  $R^2$  of the wormlike chain, which means that  $L$  and  $\lambda/L$  are coupling parameters now. In Fig. 2, we give the chemical potential, thickness and average  $\lambda_1(S)$  of tensionless bilayer with  $\chi N = 20$ ,  $R = \sqrt{6}R_g$ . Here the

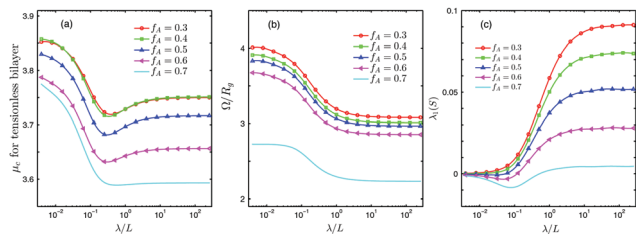


Fig. 2 The (a) chemical potential, (b) bilayer thickness and (c) average  $\lambda_1(S)$  of tensionless bilayers ( $\chi N = 20$ ,  $\eta N = 0$ ,  $R = \sqrt{6}R_g$ ).

bilayer thickness is defined as the copolymer excess per unit area,<sup>14</sup>

$$\Omega = \frac{1}{A} \int d\mathbf{r} (\phi_A^c(\mathbf{r}) + \phi_B(\mathbf{r}) - \phi_{\text{bulk}}). \quad (39)$$

The Maier–Saupe interaction between wormlike chains is turned off, *i.e.*  $\eta N = 0$ , to compare with the coil–coil/coil system. The results for  $\lambda/L \ll 1$  agrees with the coil–coil/coil system,<sup>14</sup> and the case of  $\lambda/L \gg 1$  is converging to the rod–coil/coil system. As the rigidity of wormlike chains increases, the thickness of tensionless bilayer decreases, due to the increasing liquid-crystalline order interface. It is worth to mention that the chemical potential  $\mu_c$  for tensionless bilayer has a minimum near  $\lambda/L \approx 0.3$ , *i.e.*  $L/b = L/2\lambda \approx 1.7$ . This value is near the crossover point between the rod-like behavior and the coil-like behavior.<sup>33</sup> Fig. 3 gives the bending modulus,  $\kappa_M$ , and Gaussian modulus,  $\kappa_G$ , of tensionless bilayer membranes as functions of the chain rigidity,  $\lambda/L$ . Increased the chain rigidity, the bending modulus  $\kappa_M$  decreased, and the absolute value of Gaussian modulus  $|\kappa_G|$  almost decreased as well. The limiting values of  $\kappa_M$  and  $\kappa_G$  with  $\lambda/L$  tending to zero, in agreement with the values of coil–coil bilayers. For the coil–coil bilayers, Li *et al.*<sup>14</sup> found that  $\kappa_M$ , as a function of  $f_A$ , exhibits a weak symmetry with respect to  $f_A = 0.5$ , and  $\kappa_G$  is a monotonically decreasing function of the  $f_A$  when  $f_A < 1 - \sqrt{2/\chi N}$  ( $=0.68$  for  $\chi N = 20$ ), and its value changes from positive to negative, crossing zero at around  $f_A = 0.41$ . This phenomenon is also observed for the semiflexible bilayers, however the threshold value for changing sign of  $\kappa_G$  is not exactly 0.41. As shown in Fig. 3(b),  $\kappa_G$  is close to zero when  $f_A$  is close to 0.4.

### 3.3 Influence of Maier–Saupe interaction

When the polymers contain rigid segments, the interaction between different segments increases the tendency of

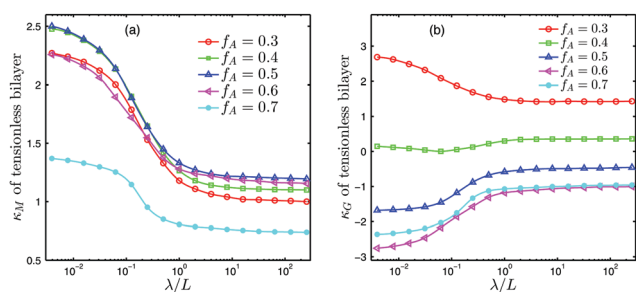


Fig. 3 The (a) bending modulus  $\kappa_M$  and (b) Gaussian modulus  $\kappa_G$  of tensionless bilayers ( $\chi N = 20$ ,  $\eta N = 0$ ,  $R = \sqrt{6}R_g$ ).

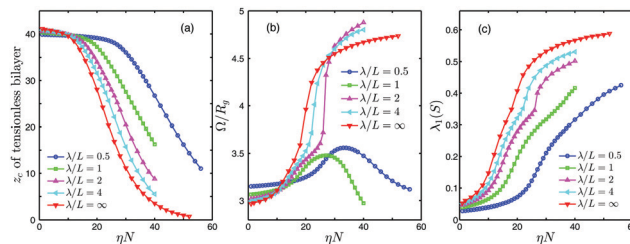


Fig. 4 The (a) chemical potential activity, (b) bilayer thickness and (c) average  $\lambda_1(S)$  of tensionless bilayers ( $R = \sqrt{6}R_g$ ,  $\chi N = 20$ ,  $f_A = 0.5$ ).

parallel arrangement. This orientational interaction is described by the Maier–Saupe interaction. Fig. 4 gives the chemical potential and order parameters of tensionless bilayer as a function of  $\eta N$ , where some typical chain rigidity,  $\lambda/L = 0.5, 1, 2, 4$  and  $\infty$ , are considered. Since the formation of liquid-crystalline phase decreases the free energy of the bilayers, the chemical potential activity  $z_c$  is decreasing when  $\eta N$  increases, meanwhile the increasing  $\lambda_1(S)$  indicates more and more strong liquid-crystalline order.

As could be seen in Fig. 4(b), the thickness of the bilayers exhibit different behaviour for  $\lambda/L \leq 1$  and  $\lambda/L \geq 2$ . This is due to the fact that the semiflexible chain of copolymer in the bilayer has different configurations which could be regarded as different liquid-crystalline phases. Furthermore, the chain rigidity affected the phase transitions. When semiflexible blocks have large chain rigidity, such as  $\lambda/L \geq 2$ , the bilayers transit from  $A_c$ -phase (interdigitated spatial arrangement) to  $A_s$ -phase (end-to-end arrangement) as  $\eta N$  increases. However, when the chain rigidity is weak, large orientation interactions lead the semiflexible blocks to be folded<sup>25,34</sup> (denoted by  $A_f$ -phase), which is reflected in the non-monotonicity of bilayer thickness  $\Omega$ .

To illustrate the influence of liquid-crystalline phases on the elastic properties of tensionless bilayers, we present the results of  $\kappa_M$  and  $\kappa_G$  as a function of  $\eta N$  in Fig. 5. When  $\lambda/L \geq 2$ , the bending modulus  $\kappa_M$  is an increasing function of  $\eta N$  and becomes very large when the bilayers possess  $A_s$ -phase. The opposite number of the Gaussian modulus  $\kappa_G$ , which are negative, have the same tendencies. However, for the bilayers possess  $A_f$ -phase when  $\lambda/L \leq 1$  and  $\eta N$  is big, the elastic properties have different tendencies, where the value of  $\kappa_M$  and  $-\kappa_G$  are decreasing functions of  $\eta N$ .

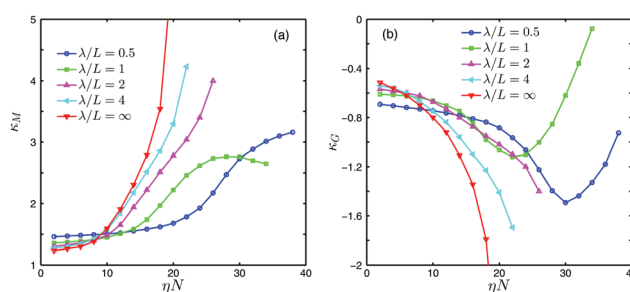


Fig. 5 The (a) bending modulus  $\kappa_M$  and (b) Gaussian modulus  $\kappa_G$  of tensionless bilayers ( $R = \sqrt{6}R_g$ ,  $\chi N = 20$ ,  $f_A = 0.5$ ).

### 3.4 Influence of temperature

It is well known that many molecular species can influence the phase state of the membrane bilayer. Temperature is however the most direct means to modulate the phase behaviour and then affect the elastic properties of the membrane bilayers. For a given copolymer, the molecular properties usually depend on the temperature. The influence of temperature in our SCF model are reflected in the parameters such as  $\lambda/L$ ,  $\chi N$  and  $\eta N$ . In this section we consider two cases of this influence. It is noted that, in principle, the effect of the various interaction parameters could be studied by changing these parameters individually. In the current study, we choose to make the variation of the interaction parameters by changing the temperature alone.

In the first case, we study the influence of temperature  $T$  on the elastic properties of tensionless bilayers by assuming that  $\chi N$ ,  $\eta N$  and  $\lambda/L$  are all proportional to the inverse of temperature  $1/T$ , *i.e.* the ratios among  $\chi N$ ,  $\eta N$  and  $\lambda/L$  are fixed. Fig. 6 gives an example of  $\chi N : \eta N : \lambda/L = 1 : 1 : 0.1$ , where the polymer contour-length  $L$  is fixed as  $4R_g$  and the chain rigidity  $\lambda/L \geq 1$ . The curves of  $\kappa_M$  are almost linear with positive slopes which indicate that the bending modulus of the bilayers are increasing functions of  $1/T$ . The dependence of  $\kappa_G$  on the temperature is much more complex, where  $\kappa_G$  changes from decreasing to increasing, crossing the minimum at a threshold value of  $1/T$ .

In the second case, we mainly study the bending modulus by assuming that the temperature only affects the chain rigidity  $\lambda/L$ , while  $z_c$  is fixed hence the bilayers are not necessarily tensionless. Fig. 7 gives an example of  $\chi N = 20$ ,  $\eta N = 16$ ,  $f_A = 0.5$ ,  $z_c = 45$ . One interesting thing is that the nonmonotonic effect of

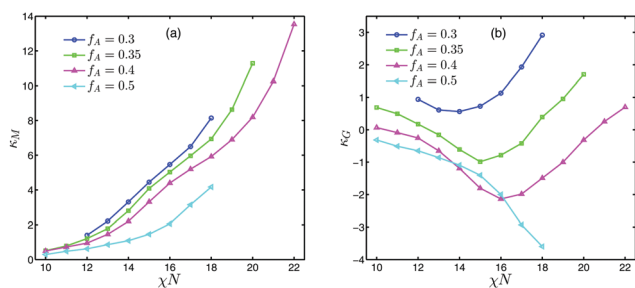


Fig. 6 The (a) bending modulus  $\kappa_M$  and (b) Gaussian modulus  $\kappa_G$  of tensionless bilayers ( $L = 4R_g$ ,  $\chi N : \eta N : \lambda/L = 1 : 1 : 0.1$ ).

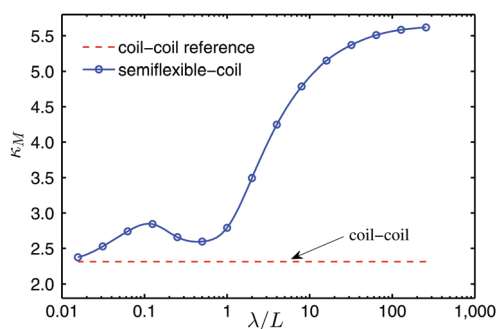


Fig. 7 The bending modulus  $\kappa_M$  of liquid-crystalline bilayers ( $R = \sqrt{6}R_g$ ,  $\chi N = 20$ ,  $\eta N = 16$ ,  $f_A = 0.5$ ,  $z_c = 45$ ).

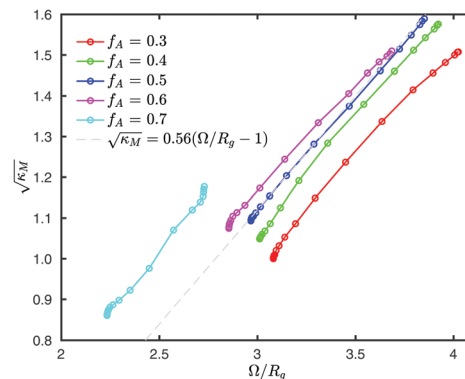


Fig. 8 Square root of the bending modulus,  $\sqrt{\kappa_M}$ , as a function of the bilayer thickness defined by the excess concentration,  $\Omega/R_g$ . (Polymer parameters are same with Fig. 3.).

temperature on  $\kappa_M$ . As mentioned before,  $\lambda/L \approx 0.3$ , corresponding to  $T \approx T_m$ , is a critical rigidity to bridge flexible and semiflexible, and the phase states on each side may be different. The bending modulus has a local minimum near  $T_m$ . This phenomenon is well known in lipid membranes<sup>5</sup> where the bending modulus decreases considerably near  $T_m$  on both sides of the transition.

### 3.5 Bilayer thickness and bending modulus

A number of studies claimed that bending modulus is proportional to the square of thickness of the membrane,<sup>6,35,36</sup>  $\kappa_M \propto d^2$ , where  $d$  is the effective membrane thickness, which could be related to the excess concentration  $\Omega$  defined in eqn (39). In Fig. 8, we give the relationship between the square root of bending modulus,  $\sqrt{\kappa_M}$ , and the excess concentration,  $\Omega$ , for the bilayers calculated in Section 3.2. The curves with different  $f_A$  are almost straight lines with almost the same slope about 0.56. Furthermore, interception of  $\Omega$  at zero  $\kappa_M$ ,  $\Omega_0$ , depends on the polymer parameters. This result confirms the scaling of  $\kappa_M$  with thickness to be nearly quadratic,  $\kappa_M \propto d^2 = (\Omega - \Omega_0)^2$ , in good agreement with existing theories<sup>6,35,36</sup> for bilayer membranes. Here we call  $d$  the effective bilayer thickness which is defined as a shift of the thickness or excess concentration  $\Omega$ , *i.e.*  $d = \Omega - \Omega_0$ . Moreover, the ratio  $C = \kappa_M/d^2$  is not sensitive to the polymer rigidity  $\lambda/L$  and the monomer volume fraction  $f_A$ . It is interesting to note that in the typical case with the A-monomer and B-monomer having the same volume fraction in the A-B copolymer, *i.e.*  $f_A = f_B = 0.5$ , the curve is extraordinarily straight and the  $\Omega$ -intercepts  $\Omega_0$  is very close to the gyration radius  $R_g$  of A-monomer, which means  $\kappa_M \propto (\Omega - R_g)^2$ .

## 4 Conclusions

In summary, we have systematically investigated the elastic properties of liquid-crystalline bilayer membranes self-assembled from semiflexible-flexible diblock copolymers. The study was carried by applying the self-consistent field theory to a molecular model composed of semiflexible-flexible diblock copolymers dissolved in corresponding flexible homopolymer solvents.

The semiflexible and flexible blocks are described by wormlike-chain and Gaussian-chain respectively. The free energy of planar, cylindrical and spherical bilayer membranes are calculated by a hybrid method, in which the orientation-dependent functions are treated using the spherical harmonics, while the special operators are discretized by the compact difference schemes. Particularly, we focused on the A-phase bilayers assuming the orientation of the semiflexible chains are perpendicular to the bilayer interface, which allows us using the symmetry of cylinder and sphere to reduce the spacial dimension to one.

The free energy of the bilayers with different geometries allowed us to obtain the elastic constants of the self-assembled bilayers. Specifically, comparing the free energy of cylindrical and spherical bilayer membranes with different curvature to the Helfrich's linear elasticity theory, we extracted the bending modulus  $\kappa_M$  and Gaussian modulus  $\kappa_G$ . These results are then used to investigate the dependence of the elastic constants of the tensionless bilayer membrane on the microscopic parameters of the system, such as the chain rigidity  $\lambda/L$  of semiflexible blocks, and the Maier-Saupe parameter  $\eta N$ . It is found that the bending modulus  $\kappa_M$  is a decreasing function of the chain rigidity  $\lambda/L$ , while the absolute value of Gaussian modulus  $|\kappa_G|$  is almost decreasing as well. The values for the flexible limit case  $\lambda/L \ll 1$  agree with the results of coil-coil/coil system. When the Maier-Saupe interaction is considered, the bilayers tend to possess liquid-crystalline order, which in turn increases the bending modulus and decreases the Gaussian modulus. However, the modulus is also affected by the configuration of semiflexible chains in bilayers, such as the case of large  $\eta N$  and small  $\lambda/L$ , where the semiflexible chains are easily folded. In addition, the influence of temperature characterized by particular parameter combinations, and the relation between the effective bilayer thickness  $d = \Omega - \Omega_0$  and bending modulus  $\kappa_M$  are examined. The results confirm the scaling of  $\kappa_M$  with the bilayer thickness to be nearly quadratic,  $\kappa_M \approx Cd^2$ , in good agreement with existing theories for bilayer membranes.<sup>6,35,36</sup> Particularly, we found that the coefficient  $C$  is not sensitive to the chain rigidity and the monomer volume fraction.

It is worth to mention that previous experiments and theory have demonstrated that semiflexible diblock copolymers could self-assembled to form a large number of liquid-crystalline bilayer phases<sup>20</sup> beyond the A-phases considered in this paper. It is natural to expect that tilt angle of semiflexible chains in bilayers could affect the elastic properties. In particular, exploring the elastic properties of C-phase bilayer membranes is a very interesting topic. Another extension of the current study is to go beyond cylindrical and spherical geometries. For instance, studies of a disk-like membrane and a pore in a planar membrane can be used to extract the line tension of the membrane edge.<sup>14</sup> However, a detailed study of these topics is beyond the scope of the current paper and we will leave this topic to future study.

## Conflicts of interest

There are no conflicts to declare.

## Acknowledgements

The authors thank National Natural Science Foundation of China (Grant No. 11421101, 11421110001 and 21790341) for financial support. ACS's research is supported by the Natural Sciences and Engineering Research Council (NSERC) of Canada. The computation was made possible by the facilities of the Shared Hierarchical Academic Research Computing Network (SHARCNET).

## References

- 1 A. Taubert, A. Napoli and W. Meier, *Curr. Opin. Chem. Biol.*, 2004, **8**, 598–603.
- 2 W. Helfrich, *et al.*, *Z. Naturforsch., C: Biochem., Biophys., Biol., Virol.*, 1973, **28**, 693–703.
- 3 Z. Tu and Z. Ou-Yang, *Adv. Colloid Interface Sci.*, 2014, **208**, 66–75.
- 4 J. Nagle, *Faraday Discuss.*, 2013, **161**, 11–29.
- 5 R. Dimova, *Adv. Colloid Interface Sci.*, 2014, **208**, 225–234.
- 6 F. M. Thakkar, P. K. Maiti, V. Kumaran and K. G. Ayappa, *Soft Matter*, 2011, **7**, 3963–3966.
- 7 A. J. Sodt and R. W. Pastor, *Biophys. J.*, 2013, **104**, 2202–2211.
- 8 M. Hu, J. Briguglio and M. Deserno, *Biophys. J.*, 2012, **102**, 1403–1410.
- 9 D. Marsh, *Chem. Phys. Lipids*, 2006, **144**, 146–159.
- 10 P.-W. Zhang and A.-C. Shi, *Chin. Phys. B*, 2015, **24**, 45–52.
- 11 B. Kheifets, T. Galimzyanov, A. Drozdova and S. Mukhin, *Phys. Rev. E*, 2016, **94**, 042415.
- 12 M. Müller and G. Gompper, *Phys. Rev. E: Stat., Nonlinear, Soft Matter Phys.*, 2002, **66**, 041805.
- 13 K. Katsov, M. Müller and M. Schick, *Biophys. J.*, 2004, **87**, 3277–3290.
- 14 J. Li, K. Pastor, A.-C. Shi, F. Schmid and J. Zhou, *Phys. Rev. E: Stat., Nonlinear, Soft Matter Phys.*, 2013, **88**, 012718.
- 15 G. Yang, P. Tang, Y. Yang and Q. Wang, *J. Phys. Chem. B*, 2010, **114**, 14897–14906.
- 16 B. D. Olsen and R. A. Segalman, *Mater. Sci. Eng., B*, 2008, **62**, 37–66.
- 17 Y.-B. Lim, K.-S. Moon and M. Lee, *J. Mater. Chem.*, 2008, **18**, 2909–2918.
- 18 J. Zhang, X.-F. Chen, H.-B. Wei and X.-H. Wan, *Chem. Soc. Rev.*, 2013, **42**, 9127–9154.
- 19 L.-Y. Shi, Y. Zhou, X.-H. Fan and Z. Shen, *Macromolecules*, 2013, **46**, 5308–5316.
- 20 Y. Cai, P. Zhang and A.-C. Shi, *Soft Matter*, 2017, **13**, 4607–4615.
- 21 G. H. Fredrickson, *The Equilibrium Theory of Inhomogeneous Polymers*, Oxford University Press, Oxford, 2006.
- 22 J. Zhou and A.-C. Shi, *Macromol. Theory Simul.*, 2011, **20**, 690–699.
- 23 P. Flory, *Principles of Polymer Chemistry*, Cornell University Press, Ithaca, New York, 1953.
- 24 W. Maier and A. Saupe, *Z. Naturforsch., A: Astrophys., Phys. Phys. Chem.*, 1958, **13**, 564–566.
- 25 W. Song, P. Tang, F. Qiu, Y. Yang and A.-C. Shi, *Soft Matter*, 2011, **7**, 929–938.

- 26 J. Yu, F. Liu, P. Tang, F. Qiu, H. Zhang and Y. Yang, *Polymers*, 2016, **8**, 184.
- 27 M. Laradji and R. C. Desai, *J. Chem. Phys.*, 1998, **108**, 4662–4674.
- 28 M. Matsen, *J. Chem. Phys.*, 1999, **110**, 4658–4667.
- 29 Q. Liang, J. Li, P. Zhang and J. Z. Chen, *J. Chem. Phys.*, 2013, **138**, 244910.
- 30 R. B. Thompson, K. O. Rasmussen and T. Lookman, *J. Chem. Phys.*, 2004, **120**, 31–34.
- 31 S. K. Lele, *J. Comput. Phys.*, 1992, **103**, 16–42.
- 32 J. C. Butcher, *Numerical Methods for Ordinary Differential Equations*, Springer-Verlag, 2nd edn, 2008.
- 33 Y. Jiang and J. Z. Y. Chen, *Phys. Rev. Lett.*, 2013, **110**, 1–5.
- 34 M. Shah and V. Ganesan, *J. Chem. Phys.*, 2009, **130**, 054904.
- 35 W. Rawicz, K. Olbrich, T. McIntosh, D. Needham and E. Evans, *Biophys. J.*, 2000, **79**, 328–339.
- 36 H. Bermúdez, D. A. Hammer and D. E. Discher, *Langmuir*, 2004, **20**, 540–543.